DOI 10.1007/s11595-017-1593-y

Effect of Deposition Time on Microstructures and Growth Behavior of ZrC Coatings Prepared by Low Pressure Chemical Vapor Deposition with the Br_2-Zr-C_3H_6-H_2-Ar System

MA Xin[1,2], LI Yong[2], MEI Min[3], HU Haifeng[2*], HE Xinbo[1], QU Xuanhui[1], CHEN Si'an[2]

(1.Institute of Powder Metallurgy, School of Materials Science and Engineering, University of Science and Technology Beijing, Beijing 10083, China; 2.Science and Technology on Advanced Ceramic Fibers and Composites Laboratory, School of Aerospace Science and Engineering, National University of Defense Technology, Changsha 410073, China; 3.Science and Technology on Advanced Functional Composites Laboratory, Aerospace Research Institute of Materials and Processing Technology, Beijing 100076, China)

Abstract: ZrC coatings were deposited on graphite substrates by low pressure chemical vapor deposition (LPCVD) with the Br_2-Zr-C_3H_6-H_2-Ar system. The effects of deposition time on the microstructures and growth behavior of ZrC coatings were investigated. ZrC coating grew in an island-layer mode. The formation of coating was dominated by the nucleation of ZrC in the initial 20 minutes, and the rapid nucleation generated a fine-grained structure of ZrC coating. When the deposition time was over 30 min, the growth of coating was dominated by that of crystals, giving a column-arranged structure. Energy dispersive X-ray spectroscopy showed that the molar ratio of carbon to zirconium was near 1:1 in ZrC coating, and X-ray photoelectron spectroscopy showed that ZrC was the main phase in coatings, accompanied by about 2.5mol% ZrO_2 minor phase.

Key words: ZrC; ultra-high temperature ceramic; microstructures; growth behaviors; chemical vapor deposition

1 Introduction

Zirconium carbide (ZrC) is one of the most promising ultra-high temperature materials due to its high melting point (3 540 ℃), chemical inertness, hardness and ablation resistance[1,2]. Chemical vapor deposition (CVD) has the advantages of high deposition rate, good adhesion between coating and substrate as well as uniform coating for complex-shaped components. A stable and exact feed of Zr-source is the crucial procedure during CVD, because the microstructures and composition of ZrC coating strongly depend on the amount of Zr-source in the system[3].

Many methods have been proposed to provide a controllable and stable Zr-source for fluidized bed during ZrC deposition, which can be classified into two categories: sublimation of zirconium halide and reaction of halide vapor with Zr-metal. The first category depends on the flow rate of carrier gas and the heating temperature of zirconium halide to control the throughput of Zr-source, accompanied by vapor condensation and agglomeration though. Thus, it fails to strictly control the flow rate of zirconium halide. Moreover, the deliquescence of zirconium halide introduces impurity elements into the reaction system during charging[4-9]. The latter category employs halogen gas or halohydrocarbon to react with Zr-metal at adequate temperature, producing zirconium halide with convenient operation and cost-competitiveness and without impurities[10-12]. Bromine has an adaptive saturated vapor pressure at room temperature and medium effects compared with those of other halogen gases. However, ZrC coatings have seldom been prepared by low pressure chemical vapor deposition (LPCVD) using the bromination process hitherto.

We have previously reported the influence of total pressure on the microstructures of ZrC coatings deposited by the Zr-Br_2-C_3H_6-H_2-Ar system[13]. In this study, the main objective was to evaluate the effect of deposition time. Phase composition and microstructure were investigated to examine the structural evolution of ZrC coating. In addition, the chemical compositions and growth behavior of ZrC coatings were clarified.

2 Experimental

2.1 Preparation of ZrC coating

ZrC coating was deposited by CVD with the

(Received: Mar. 4, 2016; Accepted: June 13, 2016)

MA Xin(马新): Ph D; E-mail: ustmaxin@163.com

*Corresponding author: HU Haifeng(胡海峰): Prof.;Ph D;E-mail: hfhu_nudt@nudt.edu.cn

Founded by the National Natural Science Foundation of China (No. 91216302) and the National Program on Key Basic Research Project of the People's Republic of China (No. 2015CB655200)

Zr-Br_2-C_3H_6-H_2-Ar system in a horizontal hot-wall apparatus. The self-made LPCVD system (Fig. 1) consisted of four main parts: a gas supply system, a bromination furnace, a deposition furnace and an exhaust system. A W-Re thermocouple was used to measure the temperature of the deposition zone, and the total pressure of the reaction chamber was maintained by a vacuum pump.

Bromine (Br_2, 99.5%) was used to react with Zr-metal particles to form $ZrBr_4$ vapor at 600°C. High-purity propylene (C_3H_6, 99.6%) was the source material for carbon. Purified hydrogen (H_2, 99.999%) was selected as the reducing agent for $ZrBr_4$ vapor, and argon (Ar, 99.999%) was used as the carrier of 0℃ Br_2 vapor and diluted gas. The CVD process of ZrC coating was controlled by chemical equilibrium and mass balance, with the key reactions described as follows[14]:

$$ZrBr_4 + H_2 \rightarrow ZrBr_x + HBr \ (x=0, 1, 2, 3) \quad (1)$$

$$C_3H_6 \rightarrow [C] + H_2 \quad (2)$$

$$ZrBr_x + [C] \rightarrow ZrC_y + xBr \ (x=0\text{-}4) \quad (3)$$

$$Br + H_2 \rightarrow HBr \quad (4)$$

where, y is the ratio of C/Zr. Clearly, the ZrC growth in CVD process should consist of the following processes: deposition of Zr-containing species ($ZrBr_x$), deposition of C-containing species ([C]) and deposition of ZrC_y by $ZrBr_x$ reaction with [C].

Table 1 Process parameters for CVD-ZrC

Deposition temperature/℃	Pressure/kPa	Volume flow rate (mL/min)			
		H_2	Dilute Ar	C_3H_6	Carrier Ar
1200	5	600	600	10	40

The substrates were made of graphite slices (1.85 g/cm^3), with a size of 3 mm × 15 mm × 20 mm. Before deposition, all specimens were firstly hand-abraded with 800$^{\#}$ grit SiC paper, then cleaned ultrasonically with acetone and dried at 393 K for 2 h. ZrC coating was deposited at 1 200 ℃, and the designed process parameters are listed in Table 1. The deposition time was 10, 20, 30, and 40 minutes, respectively.

2.2 Measurements

The crystalline phase and grain size of the matrix were determined by X-ray diffraction (Siements D-500, Germany). The microstructure of ZrC coating was observed by field emission scanning electron microscope (FESEM, HITACHI S-4800, Japan). This instrument allows for both SEM imaging and energy dispersive X-ray spectroscopic (EDS) analysis. Surface chemistry of ZrC coating was analyzed by X-ray photoelectron spectroscopy (XPS) using a Thermo ESCALAB 250 apparatus with Al Kα radiation of energy 1486.6 eV.

3 Results and discussion

3.1 Phase composition and textural structure

The XRD patterns and texture coefficients (TCs) of ZrC coatings at different deposition time are shown in Fig.2. The diffraction peaks of (111), (200), (220), (311), (222), and (400) planes correspond to ZrC phase with a face-centered cubic structure (JCPDS #35-0784). At the same time, there are also graphite-2H peaks from the substrates. As the deposition time increased, the graphite-2H peaks attenuated gradually, but the ZrC peaks were intensified. Only ZrC peaks were detected at the deposition time of 40 min, indicating that no free carbon existed in the as-prepared coatings. Narrow and sharp peaks suggest good crystallization of ZrC phase. Moreover, the peak intensities of different crystallographic planes changed significantly, so ZrC crystals had various growth orientations. The preferential orientation of ZrC crystals can be calculated by TC[15], as shown in Fig.2 (b):

$$TC_{(hkl)} \frac{I_{(hkl)} / I_{0(hkl)}}{\sum_N I_{(hkl)} / I_{0(hkl)}} \quad (1)$$

In this equation, $TC_{(hkl)}$ is TC of a given plane. I and I_0 represent the measured and standard intensities of ZrC respectively, and N is the number of reflections considered. In this study, (111), (200), (220), and (311) planes were considered. When the deposition time was less than 20 min, ZrC crystals had no obvious preferred orientation. Once the deposition time exceeded 30 min, TC of (200) plane was higher than those of other planes.

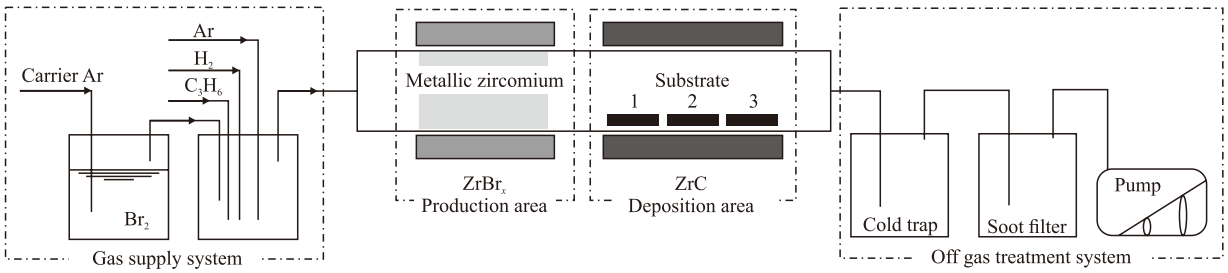

Fig.1 Schematic drawing of the CVD apparatus

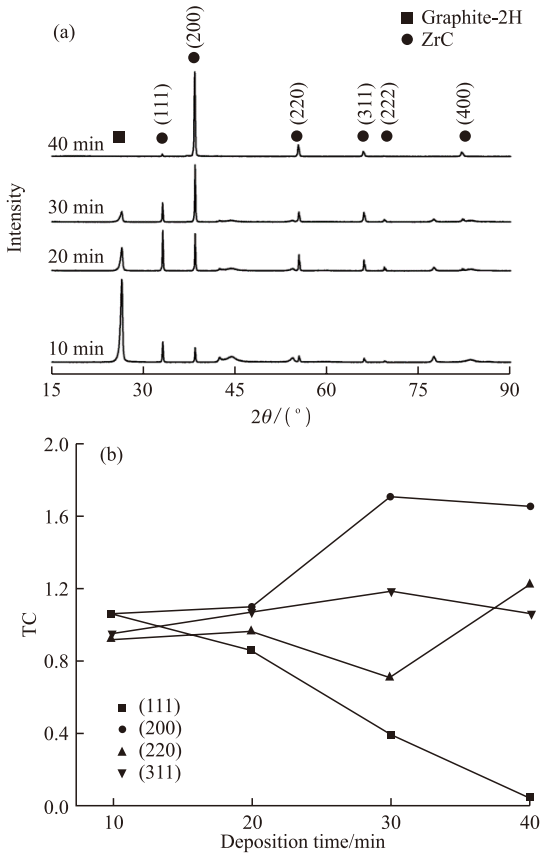

Fig.2 (a) XRD patterns and (b) texture coefficients of ZrC coatings deposited at different deposition time

3.2 Microstructures

Fig.3 shows the surface morphologies of ZrC coatings at different deposition time. The surface morphologies had significant differences. When the deposition time was 10 min (Figs.3(a) and 3(b)), the coating surface was composed of many small aggregated coral-like ZrC particles. Moreover, the loose particles had large voids owing to incomplete crystallization. When the deposition time was 20 min, the protruding ZrC particles connected with each other (Figs.3(c) and 3(d)), and the coating surface comprised island-like protuberances that were congregated tightly by nanoscale ZrC grains. As the deposition time was extended from 20 min to 30 min, ZrC grains began to grow and be stacked by numerous spherical-shaped cells (Figs.3(e) and 3(f)). In addition, large amounts of pores formed, resulting in a loose coating surface. When the deposition time was 40 min, the coating had a flat and compact surface which was stacked well-developed pyramid-like ZrC particles (Figs.3(g) and 3(h)). According to TC in Fig.2(b), ZrC coatings with a pyramid-like surface had obvious (200) preferential orientation.

In order to observe the internal microstructures of ZrC coating, the deposition time was increased to 20 h. Fig.4 shows the cross-sectional microstructure of ZrC coating deposited for 20 h. Clearly, the dense coating underwent brittle fracture and had a thickness of about 18 μm. As evidenced by the thickness of ZrC coating, the microstructure was inhomogeneous. Two distinct regions, fine-grained (I) and columnar-grained (II), were divided from the substrate/coating interface to the top surface, being in accordance with the surface morphologies of ZrC coatings at different deposition time. The formation of fine-grained coating was dominated by the nucleation of ZrC at the initial stage (Fig.4(c)), while that of column-arranged ZrC coating was dominated by crystal growth (Fig.4(b)). Notably, ZrC coating was uniform in each region without an obvious boundary between them. The stress generated from the mismatch of CTE between the coating and the substrate was effectively relieved by grain boundaries in the fine-grained region, which enhanced the coating-substrate adhesion. The columnar structure was typified by high hardness that helped resist washout under the high-speed combustion flow. In short, the structural transformation may be related to different growth behaviors of ZrC coatings deposited at different deposition time.

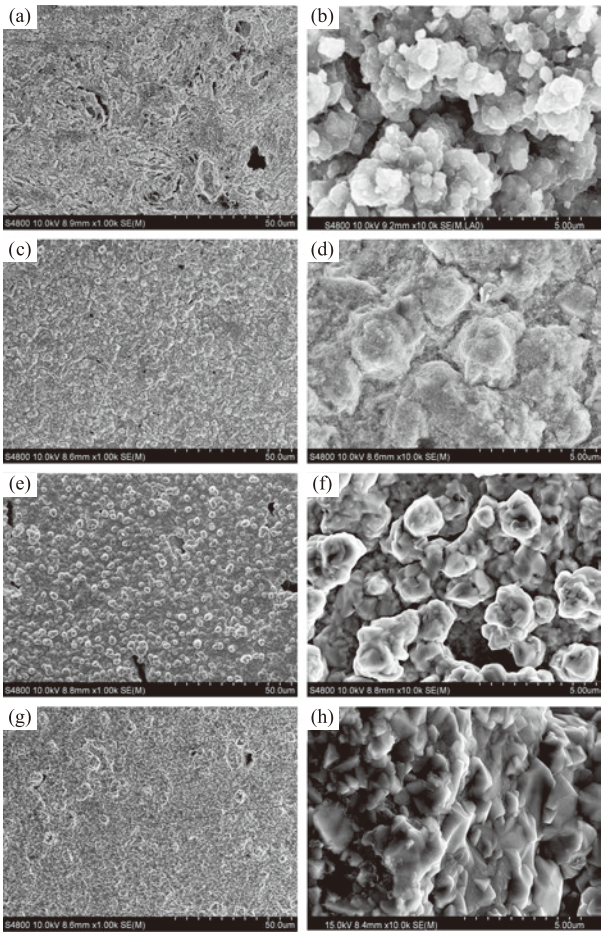

Fig.3 SEM images of the surface morphologies of ZrC coatings at different deposition time: (a) (b) 10 min; (c) (d) 20 min; (e) (f) 30 min; (g) (h) 40min

3.3 Growth behavior

The deposition mechanism can be verified by the evolutionary microstructures of ZrC coatings with prolonged deposition time. Fig.5 schematizes the

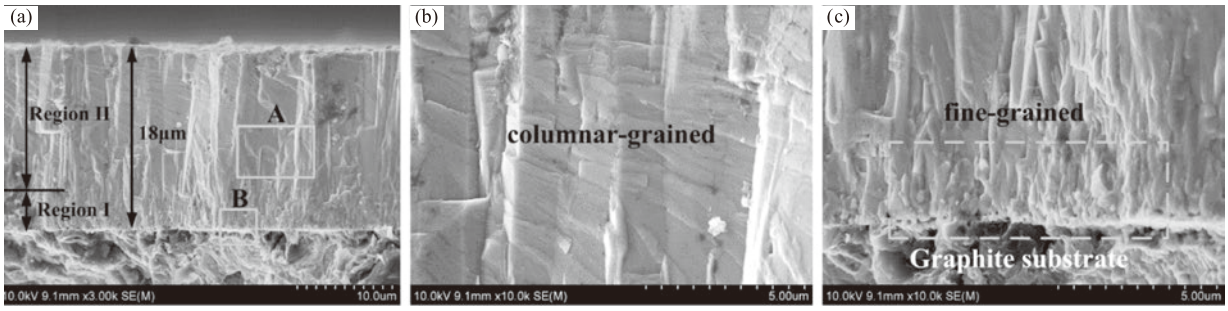

Fig.4 (a) The cross-sectional microstructure of the ZrC coating deposited for 20 h; (b) and (c) enlarged images corresponding to the regions A and B in (a) image

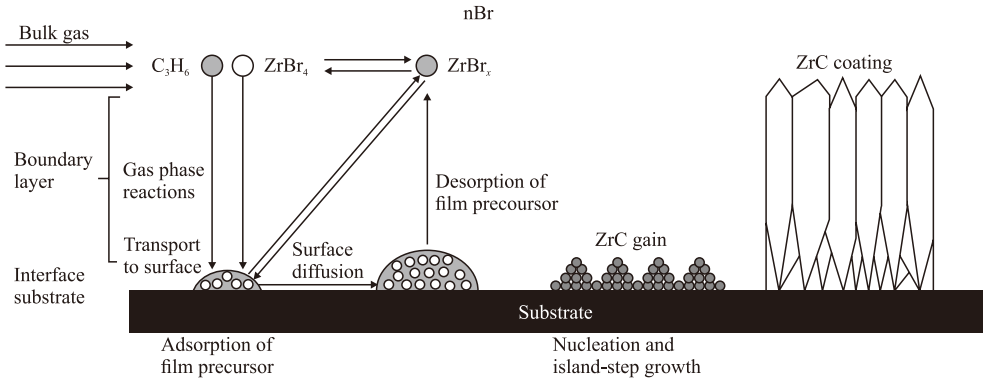

Fig.5 Schematic of ZrC coating deposition process

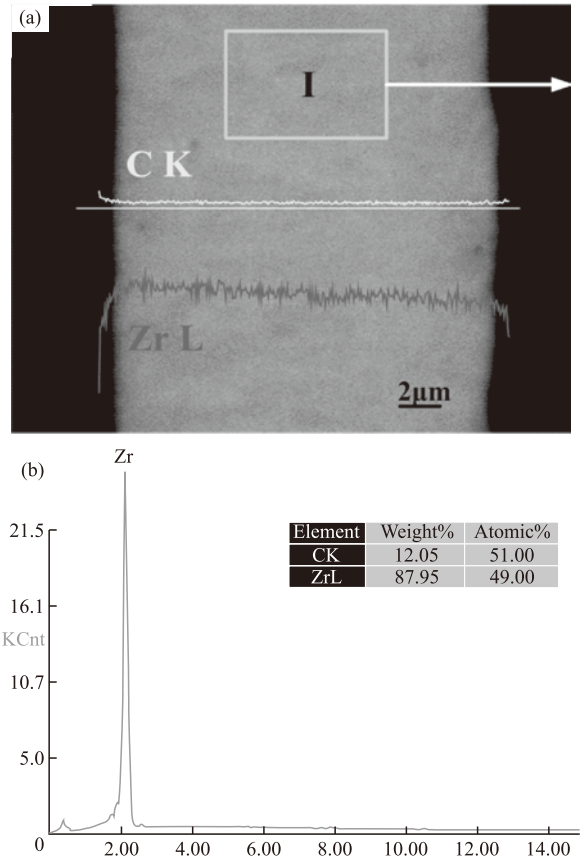

Fig.6 (a) BES cross-section images of ZrC coating; (b) EDS analysis of the region I in (a) image

deposition process of ZrC coating. The surface kinetics for ZrC growth in CVD process consisted of the following processes: deposition of carbon-containing species, deposition of hafnium-containing species and formation of carbide through reaction between the above two species. During the deposition of carbon-containing species, the gaseous hydrocarbon (C_3H_6) decomposed firstly into a liquid or plastic drop of complex organic materials, which then impinged and deposited on the substrate. Meanwhile, the reduced $ZrBr_4$ species dissolved in carbon-containing droplets and reacted with them to form ZrC clusters or islands (Fig.3(b)). The ZrC clusters or islands grew while the island density rapidly saturated, and then the islands merged through coalescence (Fig.3(d)). Coalescence decreased the island density, resulting in local denuding of the substrate where further nucleation occurred. Crystallographic facets and orientations were frequently preserved on the islands (Figs.3(f) and 3(h)) and at the interfaces between initially disoriented and coalesced particles (Fig.4(c)). Significant surface and grain boundary diffusions both occurred as the deposition time increased. Accordingly, a homogeneous columnar grain structure, from the bottom to the top of the coating, was obtained through the film thickness (Fig.4(b)).

3.4 Chemical composition

The BES cross-section images and EDS analysis of ZrC coating are shown in Fig.6. The EDS line scanning showed that the distribution of carbon and

zirconium elements was stable (Fig.6(a)), and the EDS area scanning showed that the C/Zr ratio of ZrC coating was nearly 1:1 (Fig.6(b)). In other words, a homogeneous ZrC coating was prepared by this process.

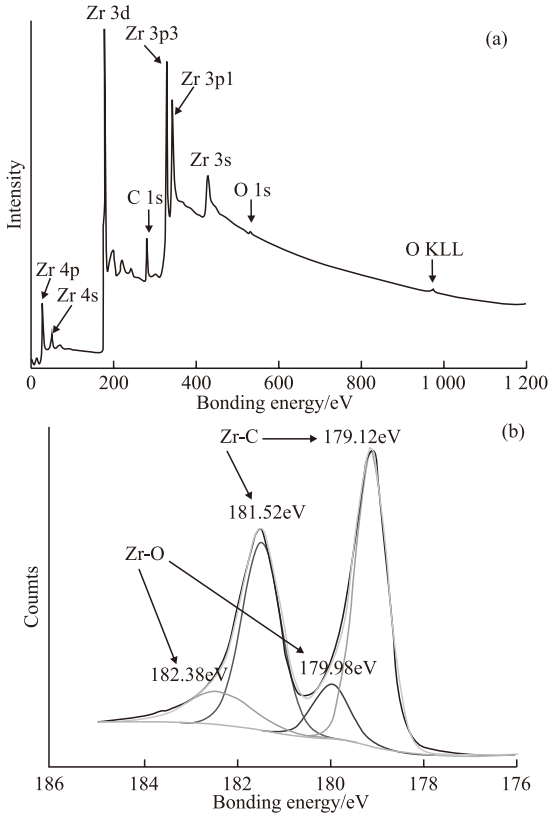

Fig.7 Survey XPS spectra of the ZrC coating (a) and the XPS fitted spectra of Zr 3d for ZrC coating (b)

ZrC coating was further characterized by XPS, a surface-sensitive analysis technology (Fig.7). Before high-resolution measurement, the samples were cleaned by Ar^+ ion sputter etching at 500 eV to remove surface oxides. Low acceleration voltage was used to minimize sputter damage. Zr, C as well as few O elements were detected. Oxygen existed due to the high affinity between Zr and O to form oxides, particularly ZrO_2, with an enthalpy of formation around -1097.46 J/mol[16, 17]. The peak corresponding to the Zr 3d band is composed of spin-orbit doublets (*i e*, Zr $3d_{5/2}$ and Zr $3d_{3/2}$), each separated by an energy difference ΔE=2.4 eV. The bonding energies of 181.52 eV and 179.12 eV correspond to Zr-C bond while those of 182.38 eV and 179.98 eV correspond to Zr-O bond. The ratios of these two kinds of bonds are 95% and 5%, respectively.

4 Conclusions

ZrC coatings were deposited on graphite substrates by LPCVD with the Br_2-Zr-C_3H_6-H_2-Ar system. The deposition time significantly affected the structural evolution of ZrC coating. ZrC grains grew in an island-layer mode, *i e*, the gaseous hydrocarbon deposited and formed liquid droplets on the substrate firstly, and then $ZrBr_4$ reacted with the organic droplets to form ZrC grains. The formation of coating was dominated by the nucleation of ZrC at the initial deposition stage, and the rapid nucleation gave the fine-grained structure of deposited ZrC coating. When the deposition time was over 30 min, the coating growth was dominated by the crystal growth, and the deposited coating exhibited a column-arranged structure. EDS showed that the molar ratio of C/Zr was near 1:1 in ZrC coatings, and the distribution of C and Zr elements was stable. XPS confirmed ZrC as the main phase in ZrC coatings, accompanied by about 2.5mol% ZrO_2 minor phase. The bonding energies of Zr-C bond for Zr $3d_{5/2}$ and Zr $3d_{3/2}$ were 181.52 eV and 179.12 eV, respectively.

Acknowledgements

The authors are grateful for the financial support by the National 973 Program of the People's Republic of China under Grant No. 2015CB655200, the National Natural Science Foundation of China (No. 91216302), Aid program for Science and Technology Innovative Research Team in Higher Educational Institutions of Hunan Province and Advanced Ceramic Fibers and Composites Innovative Research Team in National University of Defense Technology.

References

[1] Pierson HO. *Handbook of Refractory Carbides and Nitrides: Properties, Characteristics, Processing, and Applications*[M]. *New Jersey: Noyes Publications*, 1996: 55
[2] Zhao D, Zhang CR, Hu HF, *et al*. Ablation Behavior and Mechanism of 3D/ZrC Composite in Oxyacetylene Torch Environment[J]. *Compos. Sci. Technol.*, 2011, 71: 1 392-1 396
[3] Liu C, Liu B, Shao YL, *et al*. Vapor Pressure and Thermochemical Properties of $ZrCl_4$ for ZrC Coating of Coated Fuel Particles[J]. *T. Nonferr. Metal. Soc.*, 2008, 18: 728-732
[4] Liu QM, Zhang LT, Cheng LF, *et al*. Morphologies and Growth Mechanisms of Zirconium Carbide Films by Chemical Vapor Deposition[J]. *J. Coat. Technol. Res.*, 2009, 6(2): 269-273
[5] Wang SL, Li KZ, Li HJ, *et al*. Microstructure and Ablation Resistance of ZrC Nanostructured Coating for Carbon/Carbon Composites[J]. *Mater. Lett.*, 2013, 107: 99-102
[6] Jong HP, Choong HJ, Do JK, *et al*. Effect of H_2 Dilution Gas on the Growth of ZrC during Low Pressure Chemical Vapor Deposition in the $ZrCl_4$-CH_4-Ar System[J]. *Surf. Coat. Tech.*, 2008, 203: 87-90
[7] Jong HP, Choong HJ, Do JK, *et al*. Temperature Dependency of the LPCVD Growth of ZrC with the $ZrCl_4$-CH_4-H_2 System[J]. *Surf. Coat. Tech.*, 2008, 203: 324-328
[8] Sun W, Xiong X, Huang BY, *et al*. ZrC Ablation Protective Coating for Carbon/Carbon Composites[J]. *Carbon*, 2009, 47: 3 368-3 371
[9] Liu C, Liu B, Shao YL, *et al*. Preparation and Characterization of Zirconium Carbide Coating on Coated Fuel Particles[J]. *J. Am. Ceram. Soc.*, 2007, 90(11): 3690-1693
[10] Ikawa K, Iwamoto K, Ogawa T. Coating Microspheres with Zirconium Carbide-Carbon Composite by the Methylene Dichloride Process[J]. *J. Ceram. Soc. Jpn.*, 1973, 81(10): 403-406
[11] Ogawa T, Ikawa K, Iwamoto K. Effect of Gas Composition on the Deposition of ZrC-C Mixtures: the Bromide Process[J]. *J. Mater. Sci.*, 1979, 14: 125-132
[12] Ogawa T, Ikawa K, Iwamoto K. Chemical Vapor Deposition of ZrC within a Spouted Bed by Bromide Process[J]. *J. Nucl. Mater.*, 1981, 97: 104-112
[13] Ma X, Chen SA, Mei M, *et al*. Influence of Total Pressure on the Microstructures and Growth Mechanism of ZrC Coatings Prepared by Chemical Vapor Deposition from the Zr-Br_2-C_3H_6-H_2-Ar System[J]. *Ceram. Int.*, 2017, 43: 3 501-3 509
[14] Ueta S, Aihara J, Yasuda A, *et al*. Fabrication of Uniform ZrC Coating Layer for the Coated Fuel Particle of the Very High Temperature Reactor[J]. *J. Nucl. Mater.*, 2008, 376: 146-151
[15] Wang YL, Xiong X, Li GD, *et al*. Effect of Gas Composition on the Microstructure and Growth Behavior of HfC Coatings Prepared by LP-CVD[J]. *Solid. State. Sci.*, 2013, 20: 86-91
[16] Liu B, Liu C, Shao YL, *et al*. Deposition of ZrC Coated Particle for HTR with $ZrCl_4$ Powder[J]. *Nul. Eng. Des.*, 2012, 251: 349-353
[17] Chu CL, Ji HL, Yin LH, *et al*. Fabrication, Properties, and Cytocompatibility of ZrC Film on Electropolished NiTi Shape Memory Alloy[J]. *Mat. Sci. Eng. C-Mater.*, 2011, 31: 423-427